International Journal for Innovative Engineering and Management Research
PEER REVIEWED OPEN ACCESS INTERNATIONAL JOURNAL
www.ijiemr.org

COPY RIGHT

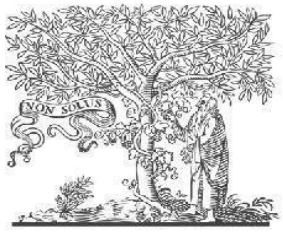

ELSEVIER SSRN

IJIEMR Transactions, online available on 5th May 2025. Link

https://ijiemr.org/downloads.php?vol=Volume-14& issue=issue05

DOI: 10.48047/IJIEMR/V14/ISSUE 05/26

Title Keratoconus Detection from Corneal Topographic Maps using Discrete Wavelet Transform and LightGBM

Volume 14, ISSUE 05, Pages: 287 – 299

Paper Authors
Prabhu Teja Geddada, Rajesh Kumar Pullagura

International Journal for Innovative Engineering and Management Research
PEER REVIEWED OPEN ACCESS INTERNATIONAL JOURNAL
www.ijiemr.org

Keratoconus Detection from Corneal Topographic Maps using Discrete Wavelet Transform and LightGBM

Prabhu Teja Geddada [1]*, Rajesh Kumar Pullagura [2]
[1,2] Department of Electronics and Communication Engineering, Andhra University, Visakhapatnam-530003, Andhra Pradesh, India.
* Corresponding author's Email: prabhuteja.rs@andhrauniversity.edu.in

Abstract
Keratoconus is a bilateral, degenerate eye disorder that affects the cornea. It is characterized by thinning and bulging of the cornea outward into the shape of a cone. It is a progressive disease if not treated early, leads to decrease in visual acuity and quality of life. Hence early diagnosis of the disease is necessary for effective treatment. This study proposes a machine learning approach for detection of keratoconus from corneal topographic maps. Discrete wavelet transform (DWT) techniques were employed for feature extraction from Pentacam-derived corneal topographic maps. Four distinct wavelet families were utilized: biorthogonal (bior1.5), reverse biorthogonal (rbio3.1), and Daubechies (db4) and haar wavelets. Each wavelet is applied with a decomposition level of four and L1 regularized Logistic Regression is used for feature selection. Light Gradient Boosting Machine (LightGBM) is used for the classification of keratoconus from corneal topographic maps derived from Pentacam instrument. Simulation results show that LightGBM has performed better on features extracted by rbio3.1 wavelet from the corneal topographic map dataset, with an overall accuracy of 87.19%, F1 score of 0.86 and AUC score of 0.96.

Keywords: Keratoconus, Corneal topographic maps, Discrete Wavelet Transform, Light Gradient Boosting Machine, Multi-class classification.

Introduction
Keratoconus is an eye disease that results in gradual thinning of the cornea leading to reduced vision [1]. Traditionally described as non-inflammatory [2], recent studies show that eyes with keratoconus have some form of inflammation [3]. Even though a bilateral disorder, one eye tends to get affected more severely than the other [4]. The disease typically manifests after puberty and progresses with a varied rate over two to three decades [5]. The advanced cases are easily diagnosed due to presence of clinical symptoms such as Munson's sign, Fleischer's Ring, Rizzuti's sign and Vogt's striae [6]. Ophthalmologists diagnose this disease based on corneal topography and tomography. These instruments capture the surface curvature of the cornea [7]. Early detection of keratoconus (KCN) is crucial as the progression of the disease can be halted or slowed with corneal collagen cross linking procedure [8]. But the early diagnosis can be challenging as disease can be asymptomatic [9]. Moreover, the diagnostic grading of subclinical KCN has not reached a global consensus [10] such that of diabetic retinopathy [11].

To address these issues many machine learning models have been proposed to aid

ophthalmologists to detect KCN. Machine learning and deep learning may provide better diagnosability and ease the burden on health care personnels when implemented as automated screening tool [12].

The main aim of this study is to evaluate the classification performance of machine learning in detecting keratoconus from corneal topographic maps obtained from the Pentacam HR instrument.

The proposed methodology employs discrete wavelet transform DWT-based feature extraction within the L*a*b* colour space. L1-penalized logistic regression is used for feature selection to enhance model interpretability by isolating the most discriminative wavelet coefficients, thereby reducing feature dimensionality. The final classification is performed using a hyperparameter-optimized LightGBM classifier.

The remainder of this paper is organised as follows: Section 2 reviews the related work on keratoconus detection and wavelet-based image analysis in medical imaging. Section 3 details the proposed methodology, including data acquisition, data preprocessing, feature extraction using DWT in L*a*b* colour space, feature selection, and the LightGBM classification framework. Section 4 presents the performance metrics, and evaluation results and experimental setup followed by a comprehensive discussion in Section 5. Finally, Section 6 concludes the paper with key findings and future research directions.

Literature Survey

In scientific literature there are numerous papers that employ machine learning algorithms in keratoconus detection H.Maile et.al [13].

Alyaa H Ali et al. [14] used image processing technique and SVM classifier to detect keratoconus from a sample size of 40 cases derived from corneal topographic maps and achieved an accuracy of 90%. Yousefi et al [15] proposed an unsupervised machine learning model for keratoconus severity identification. They have used 420 corneal parameters derived from 3156 eyes using CASIA OCT imaging systems. They have used ESI for better identification of keratoconus stages.

Lavric et al, [16] utilized 443 corneal parameters from 3136 eyes to develop machine learning model for KC detection. They implemented 25 ML models and obtained highest classification accuracy of 94% with SVM for binary classification between healthy and KCN eyes and 93% accuracy for multi-class classification between healthy, forme fruste and keratoconic eyes.

Kuo B-I et al, [17] proposed a deep learning approach for keratoconus screening using corneal topographic maps, they have achieved an AUC score of 0.995 using ResNet 152.

Ali. H Al-Timemy et al [18] developed a hybrid DL model with efficient-net b0 and SVM classifier and obtained an accuracy of 81.6% for a three-class of detecting keratoconus from corneal topographic maps.

Al-Sharify et al [19] employed decision tress and nearest neighbour analysis in classifying keratoconus based on corneal parameters and achieved an accuracy of 65.7% and 62.6% on test set.

Chaari et al [20] used an automated feature selection of corneal parameters for early keratoconus screening and achieved a highest accuracy of 98.95% and 97.08% using support vector machine (SVM) for 2 and 4 classes respectively.

International Journal for Innovative Engineering and Management Research
PEER REVIEWED OPEN ACCESS INTERNATIONAL JOURNAL
www.ijiemr.org

Kallel et al [21] used SyntEyes and GAN models to generate synthetic dataset for KC classification and achieved an accuracy ranging from 95.3% to 99.74%.

Gandhi et al [22] extracted pattern irregularities from corneal topographic maps and used transfer learning approach and have achieved a test accuracy of 77.43% on VGG19

Ahmed et al [23] used transformer based on pre trained models for KC disease detection using augmented corneal map dataset and achieved 98% accuracy with mobile net V2.

In a study done by E. Jawad et al [24] RGB to LAB colour space conversion was used to enhance the retinal image quality.

R Harikumar et al [25] proposed DWT for feature extraction from MRI images for classification between Normal and pathological cases.

S. Ryali et, al [26] used logistic regression with L1 norm regularization for feature selection and classification of fMRI data.

Materials and Methods

Data collection

In this study, 2961 corneal images gathered from 542 eyes using Oculus Pentacam are included. This dataset was made available to the research community through earlier studies [18]. The dataset used in this study consists of 3 classes 1) Keratoconus 2) Normal 3) Suspect. It was labelled as such by three corneal specialists based on standard criteria in earlier studies [18].

The keratoconus class has 1050 images. The normal class has 1050 and suspect class has 861 images. The entire dataset is split into 70% train set and 15% validation and 15% test sets. The train set contains 2072 images and validation, and test set contains 444 and 445 images respectively.

To handle class imbalance in the dataset, class weights are calculated using a balanced approach which assigns higher weights to less represented classes in the training dataset.

These computed class weights are then used to adjust loss function during model training to ensure a more balanced approach across all classes.

$$w_j = \frac{N_{\text{train}}}{C \times N_j} \qquad (1)$$

Where,

w_j is the weight for class j,

N is the total number of samples in the training set,

C is the number of classes,

N_j is the number of samples in class j in the training set.

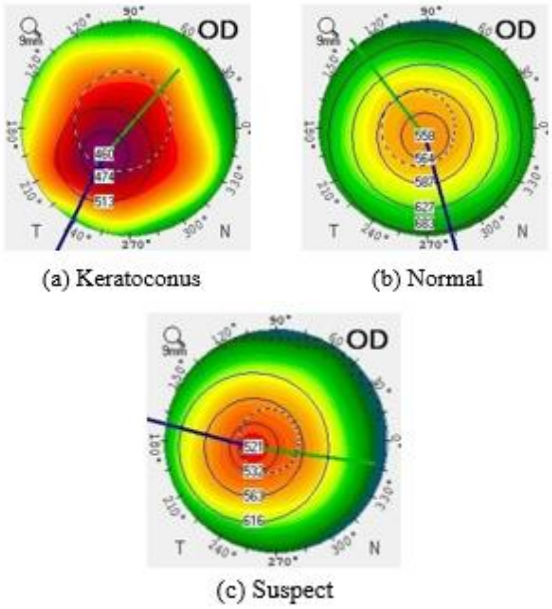

(a) Keratoconus (b) Normal (c) Suspect

Figure 1: Corneal topography images: (a) Keratoconus, (b) Normal, and (c) Suspect.

Data Preprocessing

To extract features from corneal images we first converted the images from RGB to L*a*b* colour space. L*a*b* colour space was used in previous work [19] to enhance the retinal image quality. In this work, it is used as a preprocessing step before feature extraction.

Extraction of features using wavelets

After, RGB to L*a*b* conversion, Discrete wavelets are used for feature extraction from corneal maps. Wavelets are mathematical functions that break down data into multiple frequency components, allowing each component to be analysed at a resolution suited to its scale. These functions have become essential tools for examining complex datasets. Unlike the Fourier transform, which represents an image solely based on its frequency content without spatial localization, wavelet functions maintain spatial localization. Due to its ability to represent images at multiple resolutions, the Wavelet Transform is a more effective method for extracting features from images. The wavelet-based feature extraction of medical images was implemented on brain MRI images in previous studies [25]. Four wavelet functions are used in this study namely, *bior1.5, db4, haar* and *rbio3.1*. Decomposition level for all the wavelets is set to 4.

Feature selection using L1 Logistic Regression

Feature selection is a crucial preprocessing step in machine learning (ML) that aims to reduce the dimensionality of a dataset. This process enhances model performance by improving interpretability and reducing computational costs.

Furthermore, it helps eliminate noisy or irrelevant features, which can lead to more accurate predictions. The key challenge lies in selecting the most relevant subset of features that effectively distinguishes different classes while discarding redundant or unnecessary data.

In this study we have chosen Logistic Regression with L1 regularization for feature selection as it is particularly effective in reducing dimensionality while maintaining classification performance and is able to generalize well even in the presence of many irrelevant features [26]. The solver for logistic regression is set to 'liblinear' with maximum iterations of '10,000' and the parameter 'C' is set to its default value of 1.0. Features with non-zero coefficients after model fitting were retained for further analysis, while those with zero coefficients were discarded.

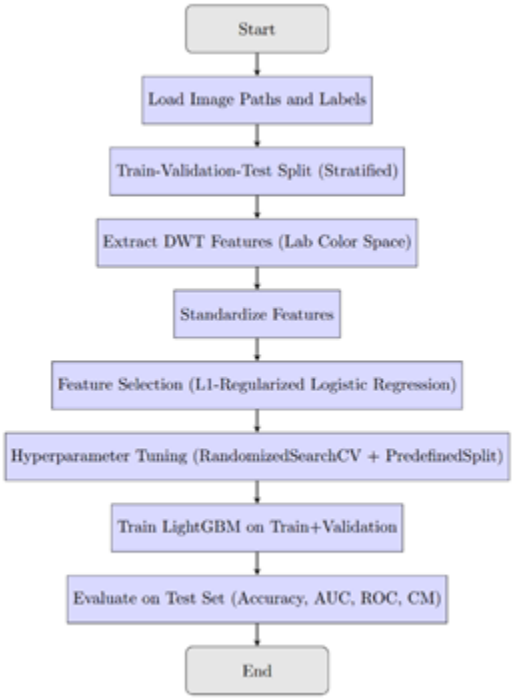

Figure 1

Figure 1. depicts the Workflow for Wavelet-Based Keratoconus Detection with LightGBM Classifier.

Light Gradient Boosting Machine

LightGBM,[27] is a comprehensive gradient boosting framework with high computational efficiency. It improves performance by computing feature histograms ahead of time. The library includes a number of

hyperparameters that allow it to adapt to various machine learning scenarios. It can be used as standard gradient boosting model while incorporating various randomization techniques like column sampling and bootstrap subsampling.

LightGBM employs a leaf-wise growth technique instead of traditional level-wise growth. In leaf wise growth, the LightGBM picks the leaf (the ending node) with the best improvement and splits it further. This ensures that the model focuses on the most important parts of the tree first. Compared to level-wise growth, this approach is faster and more efficient at reducing errors. A depth limit is added to prevent the model from growing too complex and overfit.

To optimize the performance of LightGBM classifier, a Randomized Search Cross-Validation strategy was employed. RandomizedSearchCV unlike GridSearchCV is a computationally efficient search strategy. It samples a fixed number of hyperparameter combinations from predefined distributions.

A total of 30 random combinations of hyperparameters are evaluated. Model performance is evaluated via RandomizedSearchCV using a PredefinedSplit (ps). This is being done to ensure no overlap between training and validation dataset preserving the data split integrity. The best hyperparameter combination is selected based on the performance achieved on the validation subset of 444 samples.

Table-I: Hyperparameter Search Space for LightGBM Classifier

Hyperparameter	Description	Search Range
`num_leaves`	Number of leaves in full trees	20 to 150
`max_depth`	Maximum depth of each tree	3 to 10
`learning_rate`	Step size shrinkage used in updates	0.01 to 0.2
`n_estimators`	Number of boosting iterations	50 to 500
`subsample`	Subsample ratio of training instances	0.5 to 1.0
`colsample_bytree`	Subsample ratio of columns when constructing each tree	0.5 to 1.0

Table I shows the hyperparameter search space used for LightGBM classifier tuning, specifying parameter descriptions and the respective search ranges considered during model optimization.

Performance Metrics and Evaluation Results

The entire dataset is split into 70%,15%,15% train, val and test subsets. The multi-class classification performance of LightGBM classifier is evaluated on the test subset of 445 samples with the following metrics which include accuracy, sensitivity (recall), specificity, precision and F1-score and area under receiver operating characteristic curve (AUROC). AUROC is a graphical representation of classifier's ability, with False Positive Rate (FPR) True Positive Rate (TPR) on x and y axes respectively.

$$\text{Accuracy} = \frac{TP+TN}{TP+TN+FP+FN} \quad (10)$$

$$\text{Sensitivity} = \frac{TP}{TP+FN} \quad (11)$$

$$\text{Specificity} = \frac{TN}{TN+FP} \quad (12)$$

$$\text{Precision} = \frac{TP}{TP+FP} \quad (13)$$

$$F1-score = 2 \times \frac{\text{Precision} \times \text{Recall}}{\text{Precision}+\text{Recall}} \quad (14)$$

International Journal for Innovative Engineering and Management Research
PEER REVIEWED OPEN ACCESS INTERNATIONAL JOURNAL
www.ijiemr.org

Table-II: Best Hyperparameter Settings for Each Wavelet Family with level 4 decomposition

Hyperparameter	bior1.5	db4	haar	rbio3.1
num_leaves	85	34	123	100
max_depth	8	6	7	7
learning_rate	0.0680	0.0379	0.0216	0.1525
n_estimators	333	237	149	162
subsample	0.8122	0.7280	0.8540	0.6334
colsample_bytree	0.5385	0.8059	0.5780	0.8482

Table II shows the optimal hyperparameter values for the LightGBM classifier corresponding to each discrete wavelet family used for feature extraction.These values are obtained through hyperparameter optimization using randomized search technique

Table-III: Overall performance metrics of different wavelet families with level 4 decomposition

Metric	bior1.5	db4	haar	rbio3.1
Weighted Avg. Precision	0.8551	0.8318	0.8570	**0.8729**
Weighted Avg. Recall	0.8562	0.8315	0.8539	**0.8719**
Weighted Avg. F1-Score	0.8554	0.8309	0.8539	**0.8720**
Macro Avg. Precision	0.8491	0.8242	0.8495	**0.8669**
Macro Avg. Recall	0.8498	0.8252	0.8501	**0.8679**
Macro Avg. F1-Score	0.8493	0.8240	0.8482	**0.8670**
Overall Specificity	0.9290	0.9170	0.9285	**0.9370**
Weighted Avg. AUC	0.9652	0.9567	0.9620	**0.9682**
Macro Avg. AUC	0.9635	0.9544	0.9600	**0.9665**

Table III shows the classification performance of different wavelet families based on weighted and macro averaged precision, recall, F1-score, AUC and specificity. The metrics were computed using LightGBM model for multi classification of keratoconus disease. Results show that rbio3.1 wavelet consistently outperformed other wavelets across all metrics.

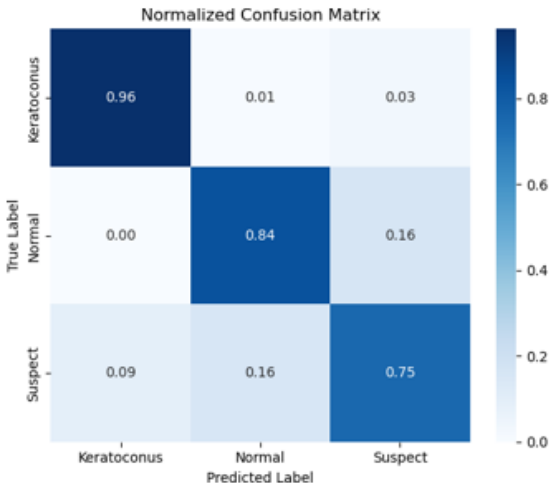

Figure 2. (a)

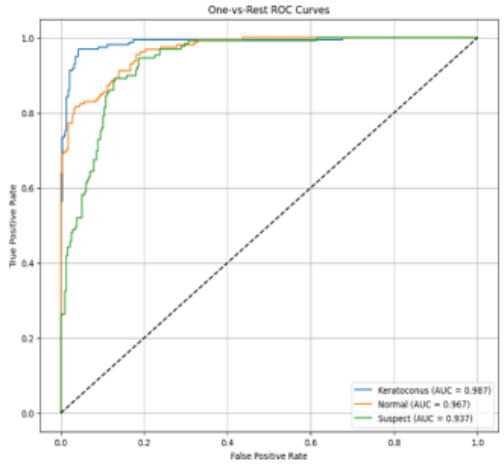

Figure 2. (b)

Figures 2 (a) and (b) show the Normalized Confusion matrix plot and ROC curve of LightGBM classifier using **bior1.5** wavelet function with decomposition level of 4

International Journal for Innovative Engineering and Management Research
PEER REVIEWED OPEN ACCESS INTERNATIONAL JOURNAL
www.ijiemr.org

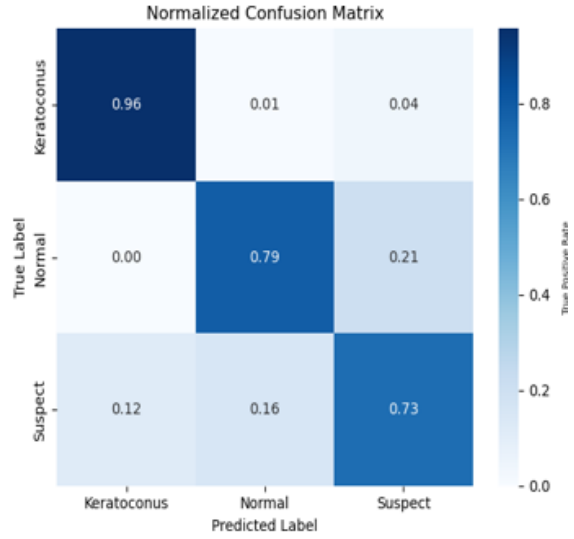

Figure 3. (a)

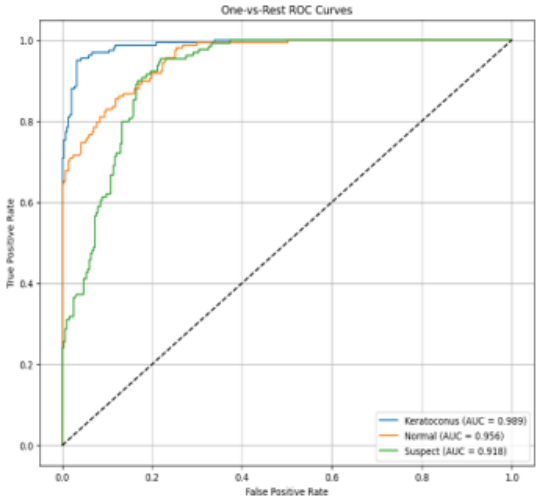

Figure 3. (b)

Figures 3 (a) and (b) show the Normalized Confusion matrix plot and ROC curve of LightGBM classifier using db4 wavelet function with decomposition level of 4

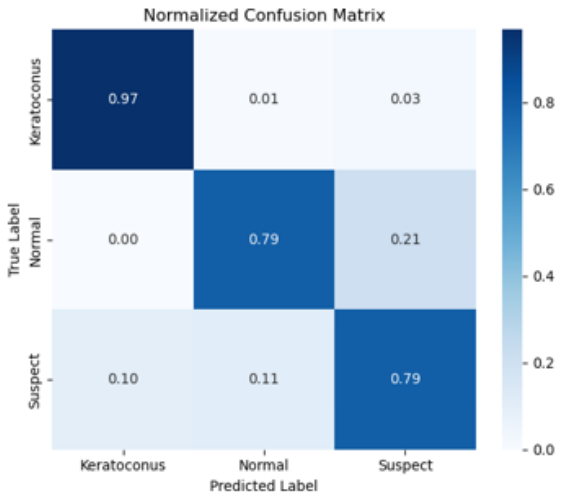

Figure 4. (a)

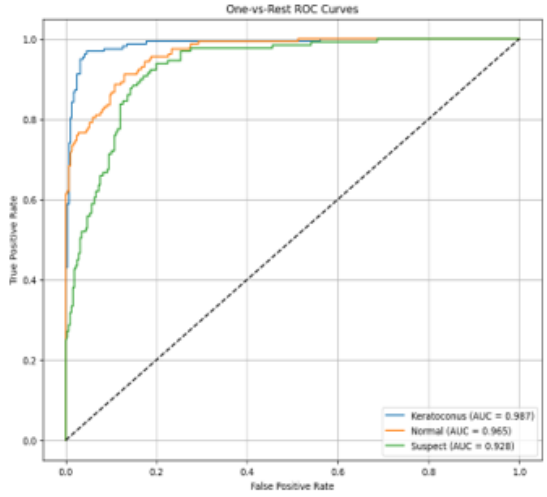

Figure 4. (b)

Figures 4 (a) and (b) show the Normalized Confusion matrix plot and ROC curve of LightGBM classifier using haar wavelet function with decomposition level of 4

International Journal for Innovative Engineering and Management Research
PEER REVIEWED OPEN ACCESS INTERNATIONAL JOURNAL
www.ijiemr.org

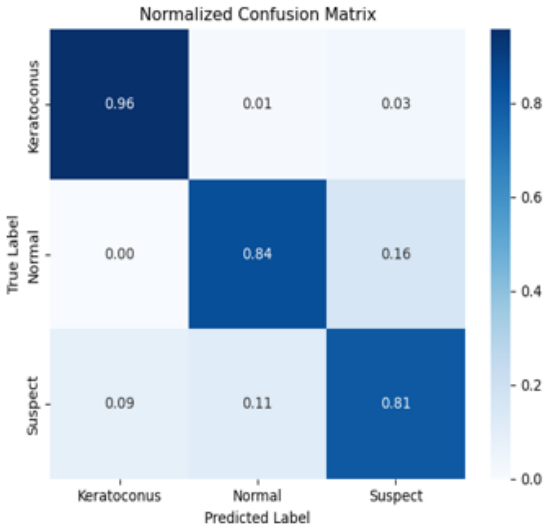

Figure 5. (a)

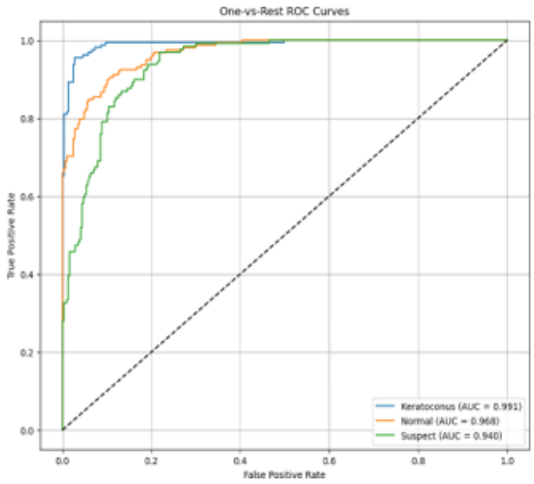

Figure 5. (b)

Figures 5 (a) and (b) show the Normalized Confusion matrix plot and ROC curve of LightGBM classifier using rbio3.1 wavelet function with decomposition level of 4

TABLE-IV: Class-wise Performance Metrics for Different Wavelet functions at level 4 decomposition

Wavelet	Class	Precision	Recall (Sensitivity)	Specificity	F1 Score	AUC (OVR)
bior1.5	Keratoconus	0.9268	0.9620	0.9582	0.9441	0.9869
	Normal	0.8627	0.8354	0.9268	0.8489	0.9667
	Suspect	0.7578	0.7519	0.9019	0.7549	0.9368
db4	Keratoconus	0.9096	0.9557	0.9477	0.9321	0.9890
	Normal	0.8562	0.7911	0.9268	0.8224	0.9563
	Suspect	0.7068	0.7287	0.8766	0.7176	0.9178
haar	Keratoconus	0.9217	0.9684	0.9547	0.9444	0.9869
	Normal	0.8929	0.7911	0.9477	0.8389	0.9647
	Suspect	0.7338	0.7907	0.8829	0.7612	0.9283
rbio3.1	Keratoconus	0.9321	0.9557	0.9617	0.9438	0.9908
	Normal	0.8926	0.8418	0.9443	0.8664	0.9684
	Suspect	0.7761	0.8062	0.9051	0.7909	0.9401

Table-IV shows the per-class performance metrics for keratoconus classification using different wavelet types for feature extraction ate level 4 decomposition. The table reports Precision, recall, Specificity, F1-Score, and Area Under the Curve (AUC) for each class.

Table-V Summary of Studies on Keratoconus Classification Techniques

Study	Classes	Dataset	Evaluation Method	Technique Used	Accuracy (%)
N. Ahmed 2024 [**23**]	3-class (KCN, Normal, Suspect)	16,016 augmented images	Train/Validation/Testing	MobileNet v2	98.00
Al-Sharify 2024 [**19**]	5-class (KCN, Normal, Suspect, Formefruste, Ectasia)	491 subjects / 8 parameters	Training/Testing	Decision Tree, Nearest Neighbor Analysis	65.7 / 62.6
Gandhi S. 2022 [**22**]	10-class (Amsler-Krumeich classification)	3962 maps with augmentation	Training/Testing	VGG19	77.43
Ali H. Al-Timemy 2021 [**18**]	3-class (KCN, Normal, Suspect)	542 eyes / 7 maps	Train/Validation/Testing	EfficientNet-B0 +SVM	81.60
This Study	3-class (KCN, Normal, Suspect)	542 eyes / 7 maps	Train/Validation/Testing	LightGBM	87.19

Table-V shows the summary of recent studies on keratoconus classification using various machine learning algorithms.The table compares the number of classes, dataset characteristics, evelaution methodologies, classification techniques, and reported performance metrics of accuracy across each study.our study has performed well, when compared to [18] provided the use of same dataset. Our method has less training and execution time due to the application of handcrafted features to train the LightGBM model.

Table-VI: Accuracy of LightGBM classifier on validation and test set with different wavelet functions.

Type of Wavelet	Decomposition Level	Accuracy (%) Validation Set	Accuracy (%) Test Set
bior1.5	4	83.11	85.62
db4	4	82.88	83.15
haar	4	83.33	85.39
rbio3.1	4	83.33	87.19

Table-VI depicts the classification performance of the LightGBM classifier using different wavelet for feature extraction at decomposition level 4. The table reports the accuracy percentages obtained on both the validation and test datasets for each wavelet.

Discussion

In this study, we developed a comprehensive machine learning pipeline for the classification of keratoconus from pentacam derived colour corneal maps using wavelet-based texture fea-tures and a LightGBM classifier. The dataset of 2961 images are divided into 70%-15%-15% stratified train, validation and test subsets to en-sure balanced representation of classes across all subsets. The train set containing 2072 images, validation set containing 444 images and test set containing 445 images. The dataset is imbalanced with suspect class being the minority. To mitigate this class weights are determined using a bal-anced method, which allocate greater weights to

classes that have fewer samples in the training set, The images are first converted into L*a*b* colour space to better capture the perceptual dif-ferences across colour channels, after which four different discrete wavelet families—Haar, Daubechies 4 (db4), Biorthogonal 1.5 (bior1.5), and Reverse Biorthogonal 3.1 (rbio3.1)—were employed for multi-scale feature extraction from corneal topography images. A decomposition level of four was chosen to comprehensively capture features across multiple spatial scales, from fine-grained local irregularities to global corneal shape deformations. Features are then standardised using 'StandardScaler' and subject-ed to feature selection using L1-regularized lo-gistic regression to mitigate redundancy and im-prove model performance. Hyperparameter op-timization is conducted through a randomized search strategy employing a predefined split cross-validation scheme combining training and validation data. The hyperparameters are tuned on the validation data to find the optimal hy-perparameters. The model is again trained on en-tire train and validation subsets with best hy-perparameter combination and is evaluated on a reserved unseen test set. In this study, LightGBM is selected as a classifier due to its high computa-tional efficiency and its ability to handle high-dimensional feature sets.

The findings of this study demonstrate the effectiveness of integrating discrete wavelet transform based feature analysis with gradient boosting models for classification of keratoconus using pentacam derived corneal topography im-ages. The hyperparameter search space outlined in Table-I is carefully selected to balance the training time and performance. The optimal hy-perparameters obtained for each wavelet family in Table-II highlight the different wavelets learn-ing dynamics. Notably, haar and rbio3.1 re-quired higher num_leaves values.The variation in optimal learning_rate from 0.0216 for haar to 0.1525 for rbio3.1 indicates differences in con-vergence behaviour.

Model evaluation metrics presented in Ta-ble-III highlights the discriminative capacity of DWT derived features. Among the wavelet fami-lies evaluated rbio3.1 consistently achieved su-perior classification performance, with a weighted average F1-score of 0.8720 and an AUC score of 0.9682. weighted average scores are calculated along with macro average score as the dataset is imbalanced. This suggests that rbio3.1 wavelet captures relevant corneal pattern irregularities more effectively than the others.

Class specific analysis in Table-IV further emphasizes the clinical relevance of these results. Detection of keratoconus cases is excellent across all wavelets with recall of 0.9684 with haar. However, performance for suspect cases remained comparatively lower with recall of 0.7287 for db4. Notably, rbio3.1 consistently outperformed other wavelets for suspect detec-tion as well, reaffirming its suitability for captur-ing subtle topographic anomalies. The figures one through four show the normalised confusion matrix plots and ROC curves of LightGBM mod-el with different wavelet functions,

When compared against existing studies in Table-V the proposed DWT-LightGBM frame-work demonstrates competitive performance. While work done in [23] reported a higher accu-racy of 98% using a MobileNet v2 based deep CNN, their study relied on over 16,000 augment-ed images, which likely contributed to improved performance. In contrast, our method achieved 87.19% accuracy using images without any aug-mentation, attesting to the effectiveness feature extraction via wavelet

decomposition. Validation and test accuracies in Table-VI, show that LightGBM model trained with rbio3.1 achieved 87.19% test accuracy, outperforming other wave-lets. Moreover, all wavelets maintained test accu-racies above 83% indicating that features extract-ed by DWT remain highly informative for kera-toconus detection. Our approach outperformed earlier works done in [18] and [23] who achieved 81.6% and 77.43% accuracy respectively using efficientnetb0+SVM and VGG19. These results are particularly notable considering lower com-putational complexity compared to deep CNNs which is crucial for deployment in real world clinical workflows. However, limitations persist. The relatively lower sensitivity for suspect class highlights the challenge of discriminating border-line ectatic changes. Additionally, while wavelet-based features offer strong interpretability, future work could explore other feature extraction tech-niques, optimizations or hybrid approaches com-bining CNN feature maps with hand crafted fea-tures.

Conclusion

This study presented a machine learning pipe-line for keratoconus classification using pen-tacam derived corneal maps, with L*a*b* colour space conversion, wavelet based feature extrac-tion and feature standardization and a LightGBM classifier. Among the four tested wavelet families, rbio3.1 achieved highest performance, with a test accuracy of 87.19%, F1-score of 0.86 and an AUC score of 0.96. The integration of L1-based feature selection and randomized hyperparameter optimization further enhanced model robustness. Compared to existing studies, our approach of-fers a computationally efficient and reliable solu-tion for automated keratoconus detection.

Conflicts of Interest

The authors declare no conflict of interest

References

[1] Y. S. Rabinowitz, “Keratoconus,” Survey of Ophthalmology, vol. 42, no. 4, pp. 297-319, Jan.-Feb. 1998, doi: 10.1016/s0039-6257(97)00119-7.

[2] J. H. Krachmer, R. S. Feder, and M. W. Belin, “Keratoconus and related non-inflammatory corneal thinning disorders,” Survey of Ophthalmology, vol. 28, no. 4, pp. 293-322, Jan.-Feb. 1984, doi: 10.1016/0039-6257(84)90094-8.

[3] V. Galvis, T. Sherwin, A. Tello, J. Merayo, R. Barrera, and A. Acera, “Keratoconus: an in-flammatory disorder?,” Eye (London), vol. 29, no. 7, pp. 843-859, Jul. 2015, doi: 10.1038/eye.2015.63.

[4] L. A. Jones-Jordan, J. J. Walline, L. T. Sinnott, S. M. Kymes, and K. Zadnik, “Asym-metry in keratoconus and vision-related quality of life,” Cornea, vol. 32, no. 3, pp. 267-272, Mar. 2013, doi: 10.1097/ICO.0b013e31825697c4.

[5] A. C. Ferdi, V. Nguyen, D. M. Gore, B. D. Allan, J. J. Rozema, and S. L. Watson, “Kera-toconus Natural Progression: A Systematic Re-view and Meta-analysis of 11,529 Eyes,” Oph-thalmology, vol. 126, no. 7, pp. 935-945, Jul. 2019, doi: 10.1016/j.ophtha.2019.02.029.

[6] U. de Sanctis, C. Loiacono, L. Richiardi, D. Turco, B. Mutani, and F. M. Grignolo, “Sensi-tivity and specificity of posterior corneal eleva-tion measured by Pentacam in discriminating keratoconus/ subclinical keratoconus,” Ophthal-mology, vol. 115, no. 9, pp. 1534-1539, 2008, doi: 10.1016/j.ophtha.2008.02.020.

[7] N. Hallett et al., “Deep Learning Based Un-supervised and Semi-supervised Classifica-tion for Kerato- conus,” in Proc. 2020 Int. Joint Conf. on Neural Networks (IJCNN), Glasgow, UK, 2020, pp. 1-7, doi: 10.1109/IJCNN48605.2020.9206694.

[8] D. M. Gore, A. J. Shortt, and B. D. Allan, “New clinical pathways for keratoconus,”

Eye (London), vol. 27, no. 3, pp. 329-339, Mar. 2013, doi: 10.1038/eye.2012.257.
[9] K. Cao, K. Verspoor, S. Sahebjada, and P. N. Baird, "Evaluating the Performance of Various Machine Learning Algorithms to Detect Subclini-cal Keratoconus," Translational Vision Science & Technology, vol. 9, no. 2, p. 24, Apr. 2020, doi: 10.1167/tvst.9.2.24.
[10] J. A. Gomes, D. Tan, C. J. Rapuano, M. W. Belin, R. Ambrosio Jr, J. L. Guell, F. Maleca-ze, K. Nishida, V. S. Sangwan, and the Global Delphi Panel of Keratoconus and Ectatic Diseas-es, "Global consensus on keratoconus and ectatic diseases," Cornea, vol. 34, no. 4, pp. 359-369, Apr. 2015, doi: 10.1097/ICO.0000000000000408.
[11] Early Treatment Diabetic Retinopathy Study Research Group, "Grading diabetic reti-nopathy from stereoscopic color fundus photo-graphs—an extension of the modified Airlie House classification. ETDRS report number 10," Ophthalmology, vol. 98, no. 5 Suppl, pp. 786-806, May 1991, PMID: 2062513.
[12] E. Korot, Z. Guan, D. Ferraz, et al., "Code-free deep learning for multi-modality medical image classi- fication," Nature Machine Intelligence, vol. 3, pp. 288–298, 2021, doi: 10.1038/s42256-021-00305-2.
[13] H. Maile, J. Li, D. Gore, et al., "Machine Learning Algorithms to Detect Subclinical Kera-toconus: Systematic Review," JMIR Medical In-formatics, vol. 9, no. 12, p. e27363, 2021, doi: 10.2196/27363.
[14] A. H. Ali, "Support Vector Machine for Keratoconus Detection by Using Topographic Maps with the Help of Image Pro-cessing Tech-niques," IOSR Journal of Pharmacy and Biologi-cal Sciences (IOSR-JPBS), vol. 12, no. 6, pp. 50-58, 2017.
[15] S. Yousefi, E. Yousefi, H. Takahashi, T. Hayashi, T. Tampo, S. Inoda, et al., "Kera-toconus severity identification using unsuper-vised machine learning," PLoS ONE, vol. 13, no. 11, p. e0205998, 2018, doi: 10.1371/journal.pone.0205998.
[16] A. Lavric, V. Popa, H. Takahashi, and S. Yousefi, "Detecting Keratoconus From Corneal Imaging Data Using Machine Learning," IEEE Access, vol. 8, pp. 149113-149121, 2020, doi: 10.1109/AC-CESS.2020.3016060.
[17] B.-I. Kuo, W.-Y. Chang, T.-S. Liao, et al., "Keratoconus screening based on deep learning approach of corneal topography," Translational Vision Science & Technology, vol. 9, no. 2, p. 53, 2020, doi: 10.1167/tvst.9.2.53.
[18] A. H. Al-Timemy, Z. M. Mosa, Z. Al-yasseri, A. Lavric, M. M. Lui, R. M. Hazarbas-sanov, and S. Yousefi, "A Hybrid Deep Learning Construct for Detecting Kerato-conus From Cor-neal Maps," TranslationalVision-Science&Technology,vol. 10,no.14,p.16,2021,doi:10.1167/tvst.10.14.6
19] Al-Sharify, N.T.; Yussof, S.;Ghaeb, N.H.; Al-Sharify, Z.T.; Naser, H.Y.; Ahmed, S.M.; See, O.H.;Weng, L.Y. Advances in Corneal Diagnos-tics Using Machine Learning. Bioengineering 2024, 11,1198.https://doi.org/10.3390/bioengineering11121198
[20] Chaari A, Fourati Kallel I, Daoud H, Omri I, Kammoun S, Frikha M. Automated feature se-lection for early keratoconus screening optimiza-tion. Biomed Phys Eng Ex-press. 2024 Dec 20;11(1). doi: 10.1088/2057-1976/ad9c7e. PMID: 39708053.
[21] Kallel, I.F., Mahfoudhi, O. & Kammoun, S. Deep learning models based on CNN architec-ture for early keratoconus detection using corneal topographic maps. Multimed Tools Appl 83, 49173–49193 (2024). https://doi.org/10.1007/s11042-023-17551-8
[22] Gandhi, Savita R., Jigna Satani, and Dax Jain. "Classification of Keratoconus Using Cor-neal Topography Pattern with Transfer Learning Approach." ICT with Intelligent

Applications: Proceedings of ICTIS 2022, Volume 1. Singa-pore: Springer Nature Singapore, 2022. 165-178.
[23] Ahmed, Nayeem, et al. "Comparative Per-formance Analysis of Transformer-Based Pre-Trained Models for Detecting Kerato-conus Dis-ease." arXiv preprint arXiv:2408.09005 (2024).
[24] E. Jawad, H. G., and H. Mohamad, "Ret-inal Image Enhancement by using Adapted His-togram Equalization based on Segmentation and Lab Color Space," International Journal of Engi-neering and Technology (IJET), vol. 15, pp. 614-622, 2022.
[25] R.Harikumar and B. Vinoth Kumar, "Per-formance analysis of neural networks for classifi-cation of medical images with wavelets as a fea-ture extractor," International Journal of Imaging Systems and Technology, vol. 25, pp. 33-40, 2015, doi: 10.1002/ima.22118.
[26] S Ryali, V Menon, Feature Selection and Classification of fMRI data using Logistic Re-gression with L1 norm regularization, Neu-roImage, Volume 47, Supplement 1, 2009, Page S57, ISSN 1053-8119,https://doi.org/10.1016/S10538119(09)702174.
[27] G. Ke, et al., "LightGBM: A highly effi-cient gradient boosting decision tree," Ad-vances in Neural Information Processing Systems, vol. 30, 2017.